Accurate 3D Reconstruction of Complex Blood Vessel Geometries from Intravascular Ultrasound Images: In Vitro Study

K.R.Subramanian†, M.J.Thubrikar‡, B.Fowler‡, M.T.Mostafavi‡ and M.W.Funk†

†*Department of Computer Science, The University of North Carolina at Charlotte, Charlotte, NC 28223, USA*

‡*Heineman Research Laboratory, Carolinas Medical Center, Charlotte, NC 28203, USA*

ABSTRACT

We present a technique that accurately reconstructs complex three dimensional blood vessel geometry from 2D Intravascular Ultrasound (IVUS) images. Biplane x-ray fluoroscopy is used to image the ultrasound catheter tip at a *few key* points along its path as the catheter is pulled through the blood vessel. An interpolating spline describes the continuous catheter path. The IVUS images are located orthogonal to the path, resulting in a non-uniform structured scalar volume of echo densities. Iso-contour surfaces are used to view the vessel geometry, while transparency and clipping enable interactive exploration of interior structures. The two geometries studied are a bovine artery vascular graft having U-shape and a constriction, and a canine carotid artery having multiple branches and a constriction. Accuracy of the reconstructions is established by comparing the reconstructions to (1) silicone molds of the vessel interior, (2) biplane x-ray images, and, (3) the original echo images. Excellent shape and geometry correspondence was observed in both geometries. Quantitative measurements made at key locations of the 3D reconstructions also were in good agreement with those made in silicone molds. The proposed technique is easily adoptable in clinical practice, since it uses x-rays with minimal exposure and existing IVUS technology.

Keywords: intravascular, ultrasound, reconstruction, catheter, visualization, graphics, x-ray.

INTRODUCTION

Intravascular Ultrasound (IVUS), with its ability to produce high resolution tomographic images of the arterial wall, is commonly used in visualizing the vascular lumen, atherosclerotic plaque and other structures. Two factors that have propelled its popularity in the catheter lab are (1) the imaging is done in real-time, and, (2) the resolution at which the vessels are imaged is superior to other technologies such as x-ray angiography, MRI or CT. The 2D cross-sectional images reveal arterial morphology, and this information is used in diagnosis and treatment.

To understand the 3D geometry of the vessel and plaque structures, it is necessary to mentally integrate the sequence of IVUS images. The task in understanding IVUS image sequences is more complex, since the vessels are usually curved, and the sequence is neither aligned nor parallel to each other. Thus, there is an important need for development of techniques that can accurately construct and visualize 3D blood vessel geometry.

Some of the earlier work on 3D reconstruction and visualization of IVUS images assumed that the vessels were straight [1, 2, 3]. More recently, biplane angiography was used to determine the curvature of the vessel [4, 5, 6, 7], and using this in conjunction with the IVUS images resulted in more accurate vessel reconstructions. Here again, two approaches were used, either track the path of the ultrasound transducer, or use the lumen centerline as an estimation of the catheter path. In [8], both approaches were used together, because the contrasting agent sometimes obscured the catheter tip. The technique also required segmentation of the lumen boundary (and other structures) prior to 3D reconstruction. Research is also underway on 3D reconstruction on IVUS images acquired in-vivo using ECG gated pullback devices [5, 9].

Our goal is to develop a new technique that is capable of rapidly generating 3D reconstructions of blood vessel geometry, allowing physicians to *interactively explore* complex arterial structures. To capture the curvature of the vessel, our technique uses biplane fluoroscopy to image the catheter tip, at a *few important points* along the length of the vessel. The point locations obtained from the x-ray images determine the path of the IVUS catheter tip in 3D. IVUS images are located along this path, resulting in a curvilinear 3D IVUS volume. The curvilinear volume takes into account the curvature of the vessel, tortuosity of the catheter's "up" vector, and differential magnification of the biplane x-rays, prior to merging the biplane and IVUS image data. After image processing operations, the volume is input to visualization algorithms [10] to generate the vessel geometry. The current implementation generates constant density contour surfaces [11] from the volume. The resulting vessel geometry can be interactively viewed and explored on graphics workstations. Cutaway and transparent views of the vessel can be generated for exploring interior structures. Experimental results from two different blood vessel geometries are presented.

Although previous work [6, 8] on 3D reconstruction of IVUS data have used methodology similar to that proposed here, our technique differs from these as follows: (1) x-rays images of the catheter tip are recorded only in an *intermittent* manner, resulting in reduced exposure to x-rays, (2) features such as vessel branches and their ostia, and stenoses are reconstructed accurately, (3) a curvilinear volume is used, reducing computation and increasing accuracy by avoiding multiple interpolations, (4) extensive results of 3D reconstructions are presented, including cutaway and transparent views of stenoses, and, (5) interactive exploration of reconstructions is facilitated via cutaway views, and by variation of vessel opacity.

We present two example vessel geometries in this work, a bovine artery vascular graft having U-shape and a constriction, and a canine carotid artery having multiple branches and a constriction. Qualitative and quantitative validation of the 3D reconstructed geometry is illustrated by comparison to silicone molds of the blood vessels, to biplane x-ray projections and to the original IVUS images.

METHODS

Data Acquisition and Preparation

Figure 1 shows the experimental scheme used to acquire the IVUS and x-ray images for constructing the 3D IVUS volume. The setup consists of a catheter based ultrasound acquisition system

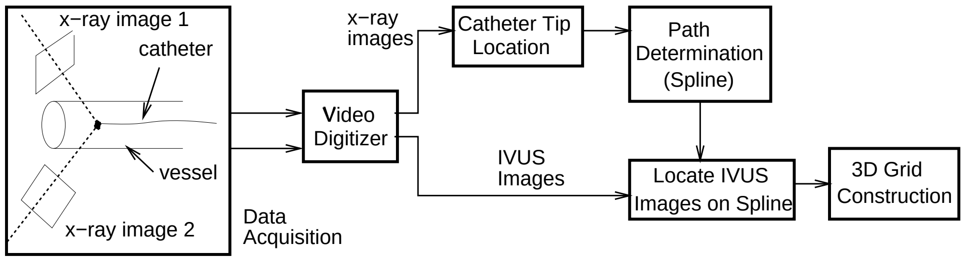

Figure 1: *3D volume construction scheme*

(Boston Scientific, Clearview Imaging System) attached to a motorized pullback system, whose speed ranges from 1 to 10 cm/minute. The x-ray images (single film exposures) are acquired using a biplane x-ray fluoroscopy apparatus. Both ultrasound and x-ray images are captured on video (SVHS). X-ray image locations are marked on echo images by an electronic trigger normally used for ECG input, and thus synchronized with the echo images. Imaging a 5 cm long vessel is usually completed within 40 to 50 seconds.

The experiment begins with the biplane x-ray machines positioned orthogonal to each other. A phantom object (we use a sphere, 11.1 mm diameter) of known size is imaged by both x-ray machines for normalizing the magnification between them. An image with the calibration marks is recorded for relating image pixels to physical units. The calibration marks are turned off during echo acquisition. Next, the ultrasound image is oriented with respect to a known reference direction. For this, a tube with a ridge at the 12 o'clock position (or facing the ceiling) is used. The echo image is rotated till the ridge appears at the 12 o' clock position. This establishes the $\vec{up}$ vector for the 3D coordinate system of the vessel. For a patient lying in a supine position, the $\vec{up}$ is in the upward (back to front) direction. All echo images are oriented with respect to this reference direction. This reference is maintained throughout the acquisition (we use a motorized pullback system, which minimizes catheter twist).

The catheter is located a few mm beyond the point at which imaging should begin, so as to eliminate any slack. Recording is begun, ultrasound imaging is started, and the pullback system is switched on. Every 2 to 3 seconds, both x-ray machines are switched on (manually by a single controlling switch) just for a moment to image the catheter tip, simultaneously an electronic signal is triggered on the echo. Once the acquisition is complete, the video recordings of the echo and x-ray images are digitized using an Abekas Diskus (Scitex Digital Video) real-time digital recorder, at 30 frames/sec. We ensure a sampling distance of 0.25 to 0.5 mm between adjacent echo images when transferring the images from the video recorder to the graphics workstation. Data volumes of varying resolutions can be generated from this image sequence. The x-ray image pairs are digitized for determining catheter tip locations followed by the phantom images and echo images with calibration marks. Figure 2 illustrates an example of echo and x-ray images.

The acquired images are at video resolution (720×486), of which the vessel occupies roughly 400×400 pixels. The images are clipped to the vessel boundaries. The smallest bounding rectangle that contains the vessel across the entire image sequence is determined and used for clipping the echo images. Next, a circular template of radius corresponding to the ring is used

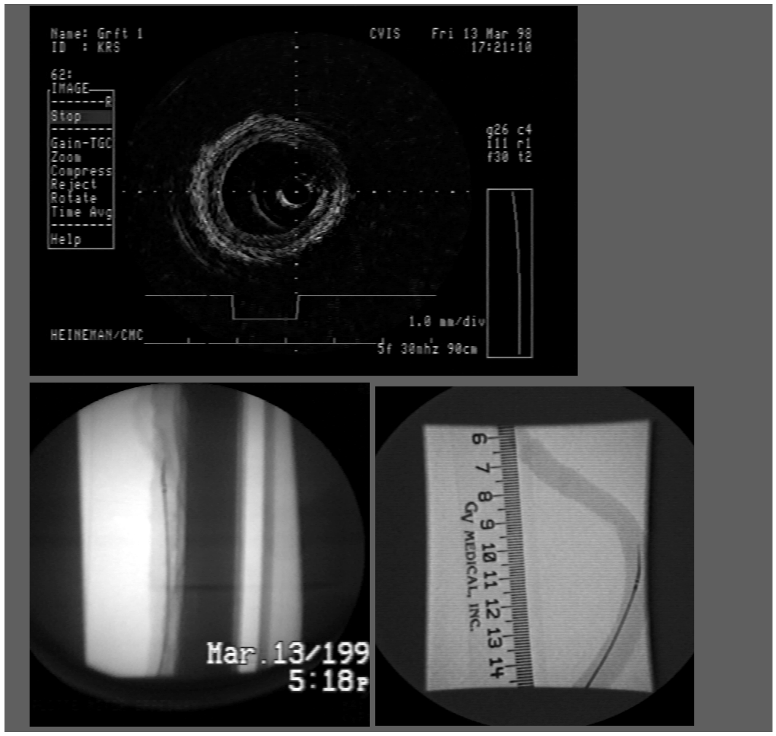

Figure 2: *Examples of IVUS and X-ray images*

to mask out the catheter. The images are then subjected to low pass filtering to compensate for noise; both Gaussian and median filters are supported. The number of images used for reconstruction and the size of each image is adjusted so as to fit within the workstation memory.

IVUS Volume Construction

Volume construction consists of determining the 3D coordinates of the catheter tip from the x-ray images, estimating the path, and locating the IVUS images along this path.

The catheter tip is located manually within each x-ray image (Figure 2). The vessel's longitudinal axis is approximately along the Z axis. The two x-ray projection images determine the (x, z) and (y, z) coordinates respectively. The sphere phantom image and the echo image with calibration marks are used in determining the scale factors for converting display pixels to physical units (mm).

The list of 3D points representing the locations of the catheter tip is normalized so that the first point becomes the origin. Next, the inter-pixel distance and the distance between adjacent images is used in converting from pixel units to physical units (mm). The catheter path is estimated by fitting an interpolating cubic spline through the points. We use the Kochanek-Bartels spline [12].

Once the catheter path has been determined, the acquired IVUS images need to be properly located along this path. Figure 3 illustrates this. $p_0, p_1, ..., p_{n-1}$ correspond to points where x-ray images have been acquired. The spline that is fitted with the $p_i s$ as the control points is then sampled uniformly, the number of sample points corresponding to the number of IVUS images to

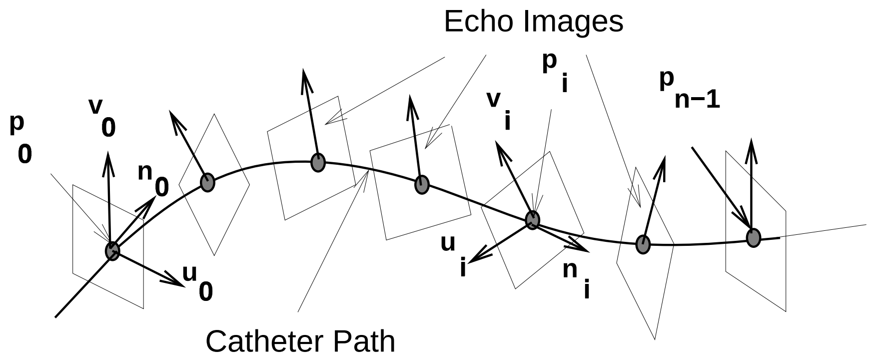

Figure 3: *Locating IVUS images.*

be used. Each IVUS image is positioned so that the catheter tip is on the spline and the image is orthogonal to the tangent vector at this point.

To orient an IVUS image on the catheter path, it is necessary to calculate two unit vectors, $\vec{u_i}$ and $\vec{v_i}$, orthogonal to the catheter path. The $\vec{v_i}s, i = 0, 1, .., n-1$ are the $\vec{up}$ vectors. The $\vec{n_i}s, i = 0, 1, .., n-1$ are the tangent vectors at each control point. The following calculations are performed to compute u_i and v_i.

$$\begin{aligned} \vec{u_i} &= \vec{n_i} \times \vec{v_{i-1}} \\ \vec{v_i} &= \vec{u_i} \times \vec{n_i} \end{aligned}$$

where $i = 1, ..., n-1$, and $\times$ indicates vector cross-product. For $i = 0$, $\vec{v_0}$, the initial $\vec{up}$ vector can be arbitrary, so long as it does not coincide with the $\vec{n_0}$). Note that $\vec{v_0}$ is not necessarily the true $\vec{up}$ vector of the first image (it is at some constant angle to it); since the succeeding images are oriented relative to each other the entire reconstruction is thus rotated with respect to the true $\vec{up}$ vector, and thus, valid. Each of the images are rotated by an amount determined by $\vec{N}_i$, which in turn is dependent on the path of the catheter tip.

Once all of the IVUS images have been properly located along the catheter path, the 3D scalar volume is determined by associating the echo intensity at all lattice points of the volume. In essence, the images are stacked along the catheter path. The 3D grid thus obtained is a non-uniform structured (hexahedral) grid, and ready for input to visualization algorithms.

RESULTS

Implementation

The current implementation of the IVUS visualization system runs on SGI Indigo-2 Unix workstations, as well as Intel PCs running Linux. We use the Visualization Toolkit (VTK) [13], for generating the 3D geometry of the vessels. OSF/Motif has been used to construct a graphical interface for all interaction and volume exploration. The main display consists of a set of menus and widgets for controlling visualization parameters, a 3D canvas where all 3D objects are displayed, and a 2D canvas that displays the original IVUS image sequence.

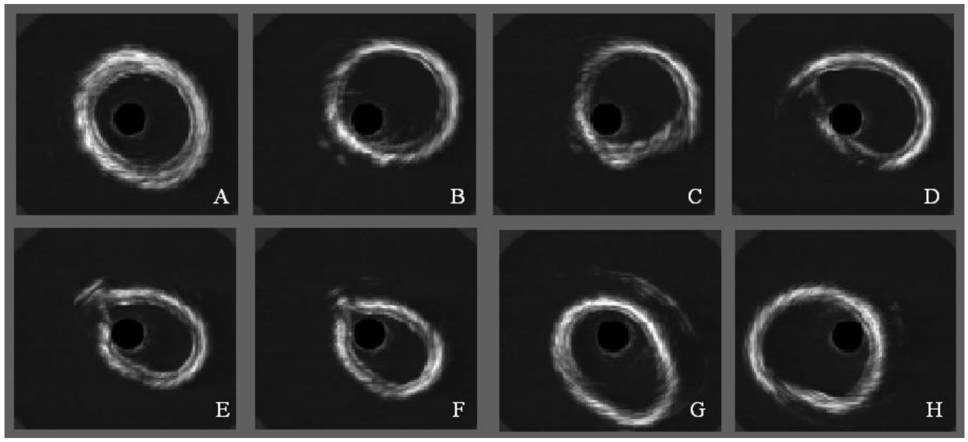

Figure 4: *Echo images along the length of the bovine artery (vascular graft). A, B, and C are prior to constriction, D is close to the constriction, E and F show the tear-drop shaped constriction, and G and H are past the constriction.*

The 2D canvas allows review of the original IVUS sequence used in the 3D reconstruction. The 3D canvas displays the reconstructed vessel as an iso-contour surface. The catheter path can also be optionally displayed. The iso-contour constant can be varied interactively to view the reconstructed surface at different contour values. Varying the opacity of the reconstruction allows a user to examine the interior structures. Alternatively, the system allows the reconstruction to be clipped to generate cutaway views of the vessel structures. Once the reconstruction has been generated (1 to 2 minutes in our examples, and dependent on volume size), it can be viewed (rotated, scaled, moved) in real-time on the SGI workstations, using hardware assisted rendering. Currently, we choose the contour surface constant interactively on a trial and error basis.

Interactive 3D picking has also been implemented to quantify vessel reconstructions. Two points can be specified on the surface of a reconstruction for calculating lengths, diameters, etc.

Examples

A number of experiments were performed to develop the IVUS reconstruction and visualization system. Each experiment resulted in acquiring several IVUS image sequences for 3D reconstruction. We illustrate results obtained from two blood vessels of different geometry.

The first specimen is a bio-polymeric vascular graft, 116 mm long. It is a conduit of bovine artery, pressure fixed (80 mm Hg) in glutaraldehyde, and covered with a dacron mesh. This specimen had a "U" shaped geometry, with a 9 mm long constriction introduced using external ties (Figures 4E, 6A). Figure 4 shows eight typical images along the length of the bovine artery; images before the constriction (A, B, C), around the bend (D), within the tear drop shaped constriction (E,F), and past the constriction and towards the end of acquisition (G,H). It may be noted that the overall geometry of the vessel cannot be understood from the IVUS images; for example, these images do not convey that the vessel is U shaped.

The second specimen is a glutaraldehyde pressure fixed (80 mm Hg) canine carotid artery, 46 mm long, which had multiple branches and a significant lumen reduction created over 4-5 mm

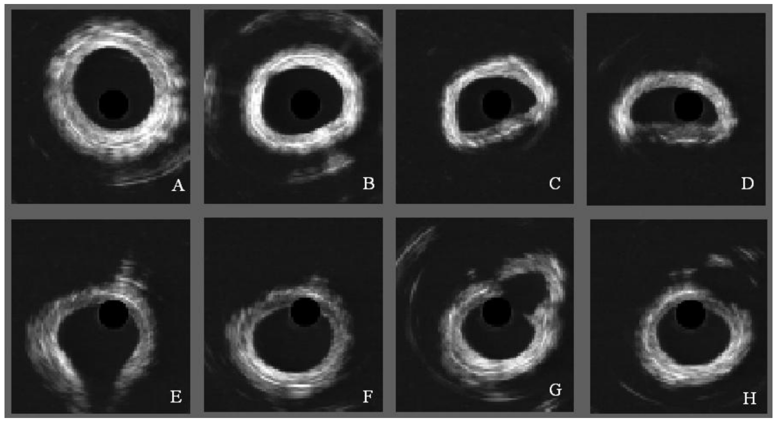

Figure 5: *Echo images along the length of the canine carotid artery. A and B are images before the constriction, C and D are within the constriction, E is the first branch, F is after the first branch, G is the second branch, H is towards the end of the vessel.*

length (Figures 5D, 7, 8). Figure 5 shows typical echo images along the carotid artery, beginning with images before the constriction (A, B), within the constriction (C, D), the first branch (E), after the branch (F), the second branch (G) and towards the end of the vessel (H). While the vessel is relatively straight in this experiment, the path of the catheter was not (as can be seen in Figure 7). Again, the echo images do not provide any clue to the complete topography of the vessel. Information offered by the 3D reconstruction is unquestionably inadequate in comparison to the echo images.

Several imaging sequences of each specimen were acquired and the sequence with the best echo images was chosen for reconstruction. The catheter tip was imaged at 21 points in the bovine artery, and 10 points in the canine artery. The number of x-ray pairs required depends upon the tortuosity of the vessel; for the two examples illustrated here, x-ray points were spaced 5 mm apart. A Scimed Ultracath 3.2F 30Mhz IVUS imaging catheter was used in the experiments. Catheter pullback speed on all runs was 1 mm/sec. Once the data acquisitions were completed, a silicone mold of each vessel at 5-10 mm Hg pressure was made for evaluating the accuracy of the 3D reconstructions.

Figure 6 illustrates the reconstruction of the bovine artery. This particular reconstruction was generated for a contour value of 43 (contour values range between 0 and 255, corresponding to 8 bit/pixel gray scale resolution). The vessel has a non-planar U shape with an introduced constriction. Figure 6A shows a view of the mold (vessel interior), illustrating the constriction, and 6B shows the vessel exterior. Figure 6C shows the same view with transparency turned on, revealing the vessel interior, and can be compared to 6A. The path of the catheter is also displayed in 6C. The images in Figures 6D, 6E and 6F correspond to another view of the artery. These figures show the U shape of the artery. It is important to note that in this view the constriction is not visible. This reinforces the value of 3D reconstructions, as they can be viewed interactively from any arbitrary view point, allowing physicians to focus on features critical to diagnosis and treatment.

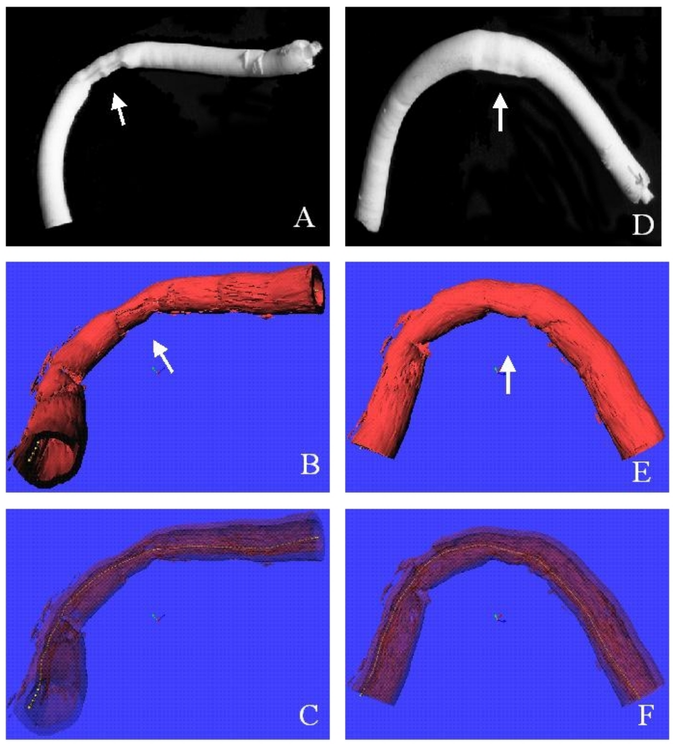

Figure 6: *Bovine artery reconstruction. A - mold of the interior of the bovine artery, B - 3D reconstruction showing vessel exterior, C - Same as B with transparency turned on to show vessel interior, D,E, and F - another view of artery showing U shape, Arrows in A,B,D and E point to the region of the externally introduced constriction. Note that the constriction is visible in view A, but not in view D. Similarly, U shape of artery is seen in D, but not in A.*

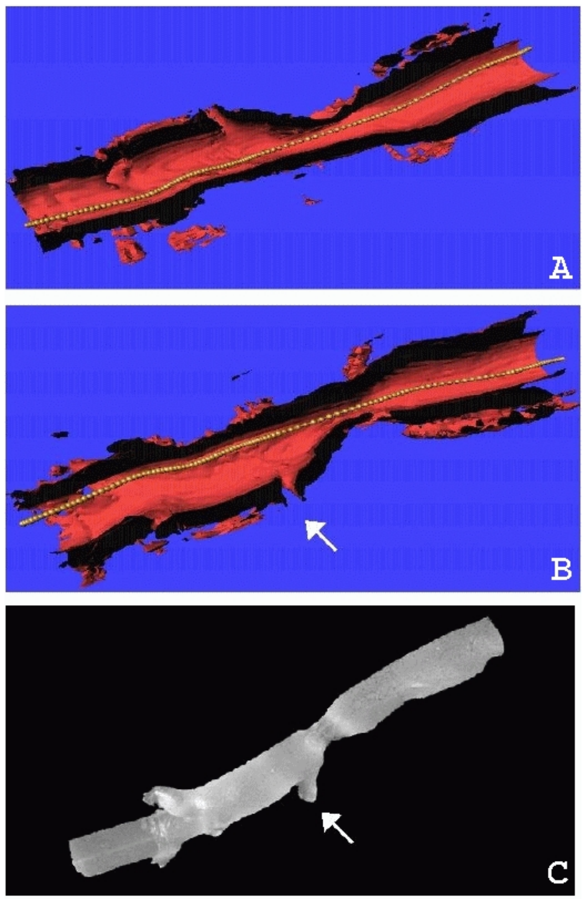

Figure 7: *Canine carotid artery reconstruction. 3 cutaway views are shown; A,B - two halves of the artery, laid one above the other, with catheter path overlaid, C - image shows a view of the silicone mold of the interior of the artery. The first branch (arrow), the ostium and the second branch is seen in the reconstruction. Topography of the entire inner surface including constriction is matched between the mold and the reconstruction.*

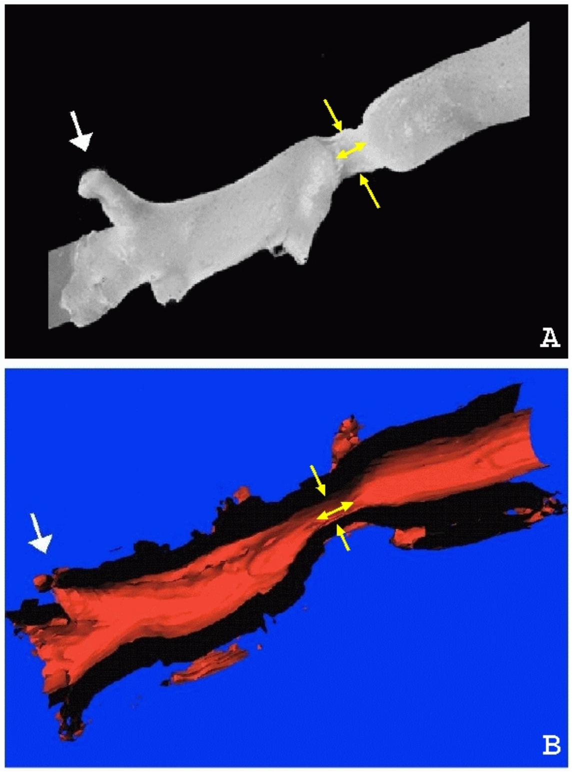

Figure 8: *Canine carotid artery reconstruction. A - second branch and its ostium (white arrow) is illustrated in the mold, B - cutaway view of reconstruction showing the second branch and its ostium (white arrow), indicating good correspondence and accuracy.*

Figure 7 illustrates cutaway views of the second vessel geometry, the canine carotid artery. This artery has 4 small branches. Figures 7A and 7B show the two halves of a cutaway, laid side by side, with the catheter path overlaid. Figure 7C shows the silicone mold of this vessel. The constriction in all its details is apparent upon reconstruction. The arrows on the middle and bottom images point to a branch and its ostium. Once again, the angle of the branch as well as the details of the ostium can be appreciated in the reconstruction.

Figure 8 illustrates another branch and the ostium; 8A shows the mold and 8B the approximately corresponding reconstruction. The branch, shown by the arrow, was also accurately reconstructed. The 3D view had to be rotated slightly to obtain the best view of this branch. In this rotated view the branch appears quite nicely in its details of the osteum, however, the width of the constriction appears smaller than that in the mold mainly because the constriction is not symmetrical around the circumference (Figure 5). The ability to capture small yet important features is a measure of the resolution and accuracy of the reconstruction system.

In Figure 9 we have oriented the reconstructed artery to correspond to the two x-ray images used in tracking the catheter tip. The coordinate system axes are illustrated by the red (X), green (Y) and blue (Z) arrows. Thus, Figure 9A shows the bovine artery oriented such that the camera is looking along the Y axis, while in Figure 9D, the camera is pointed along the X axis. Figures 9B

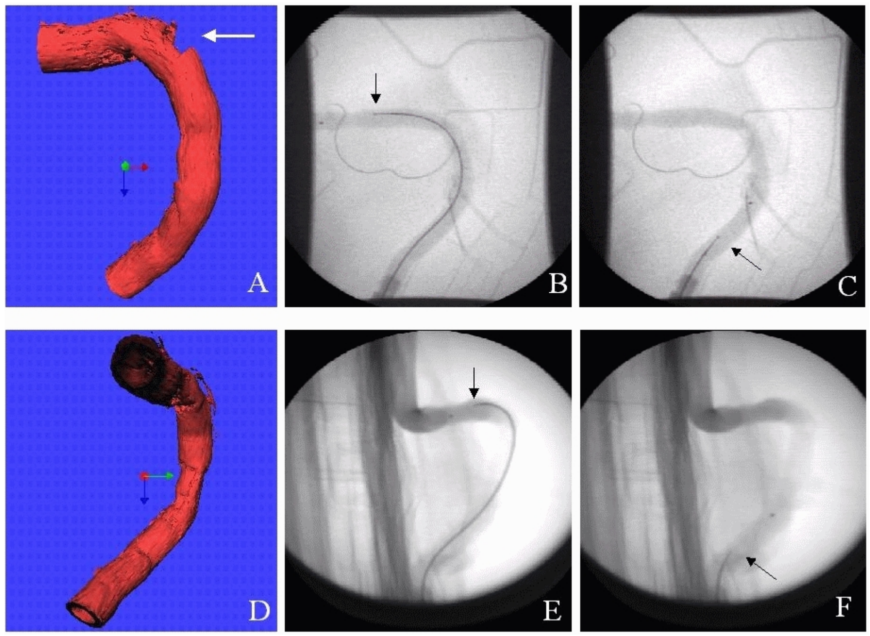

Figure 9: *Evaluating the accuracy of the bovine artery reconstruction. A - view of artery looking along the Y (green) axis, B, C - first and last x-ray images of pullback sequence in the XZ plane. D - view of the artery looking along the X (red) axis, E,F - first and last x-ray images of pullback sequence in the YZ plane. Arrows indicate the beginning and end of the catheter pullback. Artery segment between the arrows is reconstructed.*

and 9C show the first and the last x-ray images corresponding to the pullback sequence. The arrows in the x-ray images show the segment of the artery that was imaged and reconstructed. The vessel can be seen as the darker shadow surrounding the catheter. Figures 9D, 9E and 9F show the corresponding images in the YZ plane. Visual inspection of the 3D reconstructions and the x-ray images show excellent agreement in vessel shape and geometry.

Reconstruction Accuracy

Figure 10 illustrates the tear drop shaped constriction in the bovine artery; in this view, we have retained the catheter in the 3D image, for comparing the original echo images to the 3D reconstruction. Excellent correlation can be seen between the echo image and the section of the 3D reconstructed artery corresponding to the image.

The panel of images in Figure 11 shows the constriction and the first branch in the carotid artery, from the original echo images (of Figure 5) as well as the 3D reconstruction. The images in the top row show the constriction shape, while those in the bottom row show the branch. Again, excellent correspondence in shape and geometry is seen, including the branch orientation at the 2 o' clock position.

Quantitative Validation

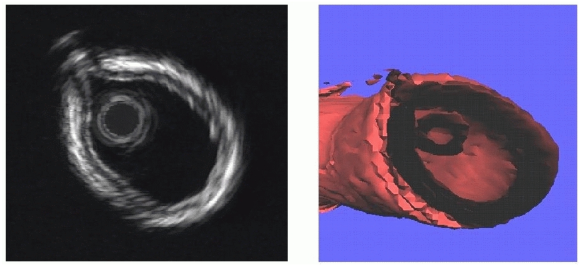

Figure 10: *Tear-drop shape constriction in bovine artery. Original echo image (left) at the constriction and the 3D reconstruction clipped and oriented to match the 2D image. Catheter ring has been retained to illustrate reconstruction accuracy. Almost a perfect correspondence is seen between the echo image and the cross-section of the reconstructed structure.*

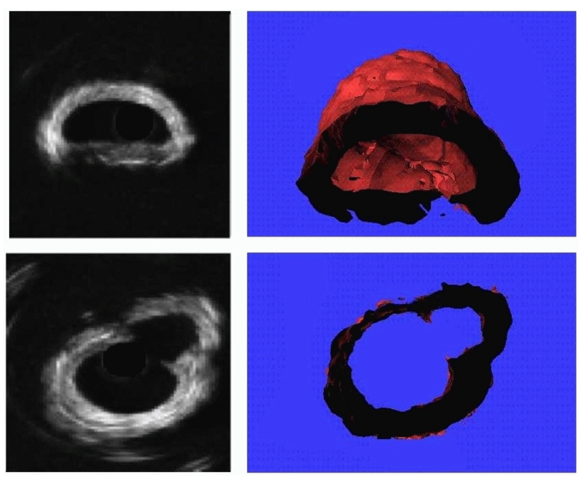

Figure 11: *Carotid Artery constriction. Upper left image shows the original echo image at the constriction and upper right image shows the corresponding view in the 3D reconstruction, clipped at the constriction. Images in the lower row show the original echo image of the branch (bottom left) and the 3D reconstruction (bottom right).*

Tables 1 and 2 shows results of quantifying the two blood vessels in comparison to their respective molds. For the bovine graft (Figure 6), the two end diameters, stenosis diameter and length and the eccentricity at the constriction (arrows) were all measured and compared to the mold. For the canine artery (Figures 7,8), the vessel length, the distance between the two branches, between each of the two branches and stenosis and the stenosis length (arrows in Figure 8B) were measured and compared to the mold. It is seen that there is very good correspondence between the reconstruction geometry and the mold.

DISCUSSION AND CONCLUSIONS

The ability to study the 3D geometry of blood vessels and plaque structures in an interactive environment is a great asset to physicians for diagnosis and treatment. We have presented a 3D reconstruction technique and a visualization system to accurately generate blood vessel geometry from 2D IVUS image sequences. We have demonstrated the accurate representation of the geometry which included complex features such as U-shape, non-symmetric constrictions, and small branches and their ostia. A key advantage of the methodology focuses on minimizing the use of x-rays, which is critical for successful adoption of the technology in clinical practice.

In-vitro reconstructions of arterial segments carried out here are very promising. Qualitative and quantitative results of comparing the 3D reconstructions to silicone molds of the vessel, as well as x-ray and the original 2D IVUS images show excellent correspondence of geometry, shape and size. The ability to capture small features such as arterial branches and their ostia, and stenoses attest to the accuracy and resolution of the system. Interactive exploration of 3D reconstructions will further enhance understanding of blood vessel structures, which is feasible on today's graphics workstations.

The current implementation requires anywhere from one to two hours of processing (after data acquisition) before 3D reconstructions can be generated and visualized. A significant amount of time is spent in digitizing and merging the data from biplane x-rays and the IVUS images. The manual inspection of the x-ray image pairs is also time consuming. Currently efforts are underway to reduce the turnaround time.

We are also in the process of extending this technique to reconstruction of blood vessels in-vivo. As illustrated from our experimental results, 3D reconstructions allow the physician to view the entire geometry of the vessel from any angle. The change in geometry due to pulsatile pressure being small (2-4%)[14], it might not be very significant in terms of diagnosis or treatment. In those instances where greater precision is required, gating can be used to minimize the reconstruction error.

The foremost advantage of this technique is the relative ease with which it can be implemented in clinical practice and, therefore, future work is focused on reducing the time of reconstruction.

ACKNOWLEDGEMENTS

This work was supported in part by the National Science Foundation under Grant No. DUE-9651080, and a grant from the American Heart Association, North Carolina Affiliate Grant-in-Aid No. B98445N.

References

[1] Rosenfield, K., Losordo, D.W., Ramaswamy, K., Pastore, J.O., Langevin, R.E., Razvi, S., Kosowsky, B.D., and Isner, J.M. 1991. Three-dimensional reconstruction of human coronary and peripheral arteries from images recorded during two-dimensional intravascular ultrasound examination. *Circulation*, 84, 1938–1956.

[2] Isner, J.M., Rosenfield, K., Losordo, D.W., and Krishnaswamy, C. 1992. Clinical experience with intravascular ultrasound as an adjunct to percutaneous revascularization. In *Intravascular Ultrasound Imaging, J.M. Tobis, P.G. Yock, Editors, Churchill Livingstone Inc., New York*, 186-197.

[3] Krishnaswamy, C., D'Adamo, A.J., and Sehgal, C.M., 1992. Three-dimensional reconstruction of intravascular ultrasound images. In *Intravascular Ultrasound Imaging, J.M. Tobis, P.G. Yock, Editors, Churchill Livingstone Inc., New York*, 141-147.

[4] Laban, M., Oomen, J.A., Slager, C.J, Wentzel, J.J., Krams, R., Schuurbiers, J.C.H, den Boer, A., von Birgelen, C., Serruys, P.W., and de Feijter, P.J.. 1995. Angus: A new approach to 3d reconstruction of coronary vessels by combined use of angiography and intravascular ultrasound. *Computers in Cardiology*, 325–328.

[5] Bruining, N., Birgelen, C.V., Mario, C.D., Prati, F., Li, W., Hoed, W.D., Patijn, M., de Feyter, P.J., Serruys, P.W., and Roelandt J.R.T.C., 1995. Dynamic 3d reconstruction of icus images based on and ecg gated pullback device. *Computers in Cardiology*, 633–636.

[6] Evans, J.L., Ng, K.H., Wict, S.G., Vonesh, M.J., Burns, W.B., Radvany, M.G., Kane, B.J., Davidson, C.J., Roth, S., Kramer, B.L., Meyers, S.N., and McPherson, D.D., 1996. Accurate three-dimensional reconstruction of ultrasound data: Spatially correct 3d reconstructions. *Circulation*, 93, 567-578.

[7] Klein, H.M., Gunther, R.W., Verlande, M., Schneider, W., Vorwerk, D., Kelch, J.,and Hamm, M., 1992. 3d-surface reconstruction of intravascular ultrasound images using personal computer hardware and a motorized catheter control. *Cardiovascular and Interventional Radiology*, 15, 97–101.

[8] Prause, G.P.M., DeJong, S.C., McKay, C.R., and Sonka, M., 1997. Towards a geometrically correct 3-d reconstruction of tortuous coronary arteries based on a biplane angiography and intravascular ultrasound. *International Journal of Cardiac Imaging*, 13, 451–462.

[9] Dhawale, P.J., Griffin, N., Wilson, D.L., and Hodgson, J.M., 1992. Calibrated 3d reconstruction of intracoronary ultrasound images with cardiac gating and catheter motion compensation. *Computers in Cardiology*, 31–34.

[10] Elvins, T., 1992. A survey of algorithms for volume visualization. *Computer Graphics*, 26, 40–47.

[11] Lorensen, W.E., and Cline, H.E., 1987. Marching cubes: A high resolution 3d surface reconstruction algorithm. *Computer Graphics*, 21, 163–169.

[12] Kochanek, D.H.U., and Bartels, R.H., 1984. Interpolating splines with local tension, continuity and bias control. *Computer Graphics*, 18, 33–41.

[13] Schroeder, W., Martin, K., and Lorensen, B., 1998. *The Visualization Toolkit: An Object-Oriented Approach to 3D Graphics*. Prentice Hall Inc., 2nd edition, 1998.

[14] Thubrikar, M.J., Roskelly, S.K., and Eppink, R.T., 1990. Study of stress concentration in the walls of the bovine coronary arterial branch. *Journal of Biomechanics*, 23, 15–26.